BER Sensitivity to Mistiming in Ultra-Wideband Impulse Radios—Part II: Fading Channels

Zhi Tian, *Member, IEEE,* and Georgios B. Giannakis, *Fellow, IEEE*

***Abstract*—We investigate timing tolerances of ultra-wideband (UWB) impulse radios. We quantify the bit-error rate (BER) sensitivity to epoch timing offset under different operating conditions, including frequency-flat fading channels, dense multipath fading channels, multiple access with time hopping, and various receiver types including sliding correlators and RAKE combiners. For a general correlation-based detector, we derived in Part I unifying expressions for the decision statistics as well as BER formulas under mistiming, given fixed channel realizations. In Part II, we provide a systematic approach to BER analysis under mistiming for fading channels. The BER is expressed in terms of the receiver's energy capture capability, which we quantify under various radio operating conditions. We also develop the optimal demodulator in the presence of timing offset and show a proper design of the correlation-template that is robust to mistiming. Through analyses and simulations, we illustrate that the reception quality of a UWB impulse radio is highly sensitive to both timing acquisition and tracking errors.**

***Index Terms*—Mistiming, optimal correlator, performance analysis, RAKE receiver, synchronization, ultra-wideband radio.**

I. Introduction

CONVEYING information over Impulse-like Radio (IR) waveforms, ultra-wideband (UWB) IR comes with uniquely attractive features: low-power-density carrier-free transmissions, ample multipath diversity, low-complexity baseband transceivers, potential for major increase in capacity, and capability to overlay existing radio frequency (RF) systems [1]–[3]. On the other hand, the unique advantages of UWB IR technology are somewhat encumbered by stringent timing requirements because the transmitted pulses are very narrow and have low power [4]. This two-part sequel quantifies the timing tolerances of UWB IR transmissions for a broad range of radio operation settings. The goal is to investigate the sensitivity to mistiming by quantifying the BER degradation due to both acquisition and tracking errors.

Manuscript received April 23, 2003; revised February 27, 2004. Z. Tian was supported by the National Science Foundation under Grant CCR-0238174. G.B. Ginnakis was supported by ARL/CTA under Grant DAAD19-01-2-011 and the National Science Foundation under Grant EIA-0324804. Parts of the work in this paper were presented at the IEEE SPAWC Conference, Rome, Italy, June 2003, and the IEEE GLOBECOM Conference, San Franscisco, CA, December 2003. The associate editor coordinating the review of this manuscript and approving it for publication was Dr. Martin Haardt.

Z. Tian is with the Electrical and Computer Engineering Department, Michigan Technological University, Houghton, MI 49931 USA (e-mail: ztian@mtu.edu).

G. B. Giannakis is with the Electrical and Computer Engineering Department, University of Minnesota, Minneapolis, MN 55455 USA (e-mail: georgios@ece.umn.edu).

Digital Object Identifier 10.1109/TSP.2005.845485

In Part I [5], we derived a unifying signal model for analyzing the detection performance of correlation-based receivers. Selecting different values for the model parameters led to various operating conditions in terms of channel types, time-hopping codes, and receiver structures. For pulse amplitude modulation (PAM) transmissions under various operating conditions, [5] analyzed the BER degradation induced by mistiming under fixed channel realizations. In fading channels, the instantaneous BER derived in [5] can be integrated over the joint probability density function (pdf) of the random channel parameters to obtain the average BER, which is the focus of this paper (Part II).

We first lay out a procedure for evaluating the BER performance of an optimum symbol-by-symbol receiver for any random channel. The BER is expressed in terms of the receiver's energy capture capability. The results depend on a couple of key channel statistics that can be numerically obtained by averaging over a large number of channel realizations. This general approach to BER analysis applies to any channel fading type but requires computationally intensive numerical evaluation. This motivates our focus on real-valued Gaussian fading channels, for which we derive closed-form BER for any RAKE receivers, expressed with respect to the channel statistics and the RAKE parameters. The energy capture capability of correlation-based receivers is quantified and tabulated for various radio operating conditions. Even though a realistic channel may follow other fading characteristics [6]–[9], the results here provide meaningful implications on the robustness of correlation-receivers to mistiming under different system settings.

The rest of this paper is organized as follows: The ensuing Section II briefly summarizes the system model presented in [5]. Section III studies the average BER performance of an optimum symbol-by-symbol detector under general fading channels, whereas Section IV derives closed-form BER expressions under Gaussian fading channels. The derivations also suggest an (optimal) correlator receiver design strategy that is robust to mistiming. Results for pulse position modulation (PPM) are summarized in Section V. Corroborating simulations are provided in Section VI, followed by concluding remarks in Section VII.

II. Signal Model

In UWB impulse radios, every information symbol is transmitted using N_f pulses over N_f frames (one pulse per frame of duration T_f). Every frame contains N_c chips, each of duration $T_c = T_f/N_c$. The equivalent transmit filter is $p_s(t) = \sum_{j=0}^{N_f-1} p(t - jT_f - c_jT_c)$ of symbol duration $T_s := T_fN_f$,

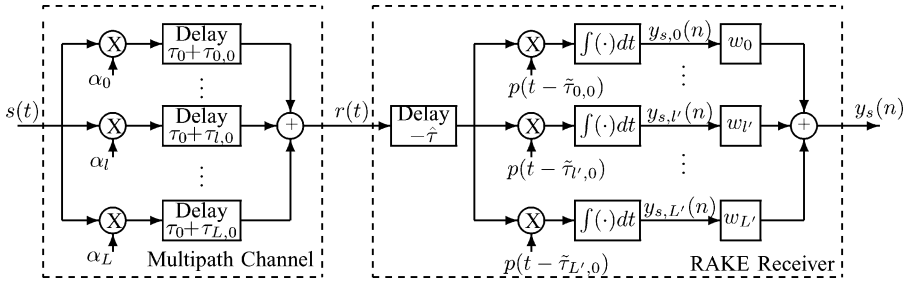

Fig. 1. Correlation-based receiver.

where $p(t)$ is an ultra-short (so-called monocycle) pulse of duration $T_p(\ll T_f)$ at the nano-second scale, and the chip sequence $\{c_j\}$ represents the user's pseudo-random time-hopping (TH) code with $c_j \in [0, N_c-1]$, $\forall j \in [0, N_f-1]$. By setting $\int p^2(t)dt = 1/N_f$, $p_s(t)$ is scaled to have unit energy. With information-bearing binary PAM symbols $s(k) \in \{\pm 1\}$ being independent identically distributed (*i.i.d.*) with zero mean and average transmit energy per symbol $\mathcal{E}_s$, the transmitted pulse stream is

$$u(t) = \sqrt{\mathcal{E}_s}\sum_{k=0}^{\infty} s(k)p_s(t - kN_fT_f). \tag{1}$$

After propagating through a multipath channel, the received signal takes on the general form

$$\begin{aligned} r(t) &= \sum_{l=0}^{L} \alpha_l u(t-\tau_l)+v(t) \\ &= \sqrt{\mathcal{E}_s}\sum_{l=0}^{L}\alpha_l \sum_{k=0}^{\infty} s(k) \sum_{i=0}^{N_f-1} p\,(t-kN_fT_f-iT_f \\ &\qquad -c(i)T_c-\tau_l)+v(t) \end{aligned} \tag{2}$$

where $(L+1)$ is the total number of propagation paths, each with gain α_l being real-valued with phase shift 0 or π and delay τ_l satisfying $\tau_l < \tau_{l+1}$, $\forall l$. The channel is random and quasi-static, with $\{\alpha_l\}_{l=0}^{L}$ and $\{\tau_l\}_{l=0}^{L}$ remaining invariant within one symbol period but possibly changing independently from symbol to symbol. The additive noise term $v(t)$ consists of both ambient noise and multiple-access interference (MAI) and is independent of $s(k)$, $\{\alpha_l\}_{l=0}^{L}$, and $\{\tau_l\}_{l=0}^{L}$. We focus on performance evaluation of the desired user, treating the composite noise $v(t)$ as a white Gaussian random process with zero-mean and power spectral density $\mathcal{N}_o/2$.

To isolate the channel delay spread, we define relative path delays $\tau_{l,0} := \tau_l - \tau_0$ for $l \in [0, L]$; the maximum delay spread is thus $\tau_{L,0}+T_p$. We select $T_f \geq \tau_{L,0}+2T_p$ and set either $c(N_f-1) = 0$ or $c(N_f-1) \leq c(0)$ to avoid inter-symbol interference (ISI) when perfect timing can be acquired. With these definitions, the composite channel formed by convolving the physical channel with the pulse is given by $h(t) := \sum_{l=0}^{L}\alpha_l p(t-\tau_{l,0})$, and the equivalent received symbol-waveform of duration T_s can be expressed as $h_s(t) := \sum_{j=0}^{N_f-1} h(t - jT_f - c_jT_c) = \sum_{l=0}^{L}\alpha_l p_s(t-\tau_{l,0})$, which simplifies $r(t)$ to

$$r(t) = \sqrt{\mathcal{E}_s}\sum_{k=0}^{\infty} s(k)h_s(t-kT_s-\tau_0)+v(t). \tag{3}$$

A correlation-based receiver correlates $r(t)$ with a locally generated correlation-template $p_s^{(rc)}(t)$, time-shifted by a nominal propagation delay $\hat{\tau}$, to produce the sufficient statistic for symbol detection

$$y(n) = \int_{nT_s+\hat{\tau}}^{(n+1)T_s+\hat{\tau}} r(t)p_s^{(rc)}(t-nT_s-\hat{\tau})dt. \tag{4}$$

We select the correlation-template $p_s^{(rc)}(t)$ to represent a generic RAKE receiver with $(L'+1)$ fingers, as shown in Fig. 1. The RAKE tap delays $\{\tilde{\tau}_{l',0}\}_{l'=0}^{L'}$ are design parameters that could be, but are not necessarily, chosen among the channel path delays $\{\tau_{l,0}\}_{l=0}^{L}$. A full RAKE arises when $L' = L$, and each $\tilde{\tau}_{l',0}$ is matched to one of the delayed paths, while $L' < L$ corresponds to a "partial RAKE," which may be less effective in energy capture but is computationally more affordable. In particular, the sliding correlator can be considered as a "RAKE-1" receiver with $L'+1 = 1$ [9]. The RAKE weights $w_{l'}$ can be selected to represent maximum ratio combining, equal-gain combining, or other linear combining techniques. For all these combiners, the correlation template $p_s(t)$ in (4) is replaced by $p_s^{(rc)}(t) = \sum_{l'=0}^{L'} w_{l'}p_s(t-\tilde{\tau}_{l',0})$.

Let us denote the timing mismatch as $\tau := \tau_0 - \hat{\tau} = N_\epsilon T_f + \epsilon$, where $N_\epsilon \in [0, N_f-1]$, and $\epsilon \in [-T_p, T_f-T_p)$. The parameters $N_\epsilon T_f$ and ϵ indicate the breakdown of mistiming into *acquisition* and *tracking* errors, respectively. Notice that N_ϵ is limited to N_f finite values since timing is resolvable only within a symbol duration. Defining the normalized auto-correlation function of $p(t)$ as $R_p(\tau) := N_f\int_{-\infty}^{\infty} p(t)p(t-\tau)dt \in [-1, 1]$, we combine (2) and (4) to reach a unifying expression for the detection statistic [5]

$$y(n) = \sqrt{\mathcal{E}_s}\sum_{k=0}^{\infty} s(k) \sum_{i=0}^{N_f-1}\sum_{j=0}^{N_f-1}\sum_{l=0}^{L}\sum_{l'=0}^{L'} w_{l'}\alpha_l \frac{R_p(\Lambda_p)}{N_f} + v(n) \tag{5}$$

where $\Lambda_p := (k-n)N_fT_f+(i-j)T_f+(c(i)-c(j))T_c+N_\epsilon T_f+\epsilon+\tau_{l,0}-\tilde{\tau}_{l',0}$. For convenience, let $y_s(n) := y(n)-v(n)$ represent the noise-free (signal) component of the decision statistic. When the RAKE taps are normalized by $\sum_{l'=0}^{L'} w_{l'}^2 = 1$, the noise term $v(n)$ is Gaussian with zero mean and variance $\sigma_v^2 = (\mathcal{N}_o/2)$. Equation (5) subsumes various operating conditions in terms of channel types (L, $\{\alpha_l\}$, and $\{\tau_l\}$), TH codes ($\{c_j\}$), and receiver structures (L', $\{w_{l'}\}$, and $\{\tilde{\tau}_{l'}\}$).

In Part I [5], we derived a unifying BER expression under mistiming for fixed channel realizations. Conditioned on $(s(n)=1,\ s(n-1)=\pm 1)$, $y_s(n)$ in (5) can be expressed as $y_s(n)|(1,1)=\sqrt{\mathcal{E}_s\mathcal{E}_\alpha(\epsilon|\{\alpha\}_{l=0}^L)}$, when two consecutive binary symbols have the same sign, or $y_s(n)|(1,-1)=\sqrt{\mathcal{E}_s\mathcal{E}_\alpha(N_\epsilon,\epsilon|\{\alpha\}_{l=0}^L)}$, where there is a change of symbol signs. Here, $\mathcal{E}_\alpha(N_\epsilon,\epsilon|\{\alpha\}_{l=0}^L)$ denotes the portion of symbol energy that is collected by a receiver under both acquisition and tracking errors, whereas $\mathcal{E}_\alpha(\epsilon|\{\alpha\}_{l=0}^L)$ denotes the received energy subject to tracking error only, noting that transmission of two identical consecutive symbols reduces the impact of acquisition errors on $y_s(n)$. Thus, the instantaneous BER is given by [5]

$$\begin{aligned}P_e\left(N_\epsilon,\epsilon|\{\alpha_l\}_{l=0}^L\right)&=Pr\left(y(n)<0|s(n)=1\right)\\&=\frac{1}{2}Pr\left(y(n)<0|(1,1)\right)\\&\quad+\frac{1}{2}Pr\left(y(n)<0|(1,-1)\right)\\&=\frac{1}{2}Q\left(\sqrt{\frac{2\mathcal{E}_s\mathcal{E}_\alpha\left(\epsilon|\{\alpha_l\}_{l=0}^L\right)}{\mathcal{N}_o}}\right)\\&\quad+\frac{1}{2}Q\left(\sqrt{\frac{2\mathcal{E}_s\mathcal{E}_\alpha(N_\epsilon,\epsilon|\{\alpha_l\}_{l=0}^L)}{\mathcal{N}_o}}\right).\end{aligned}\tag{6}$$

III. BER Sensitivity Under General Fading

Focusing on symbol-by-symbol optimum reception,[1] we now lay out a procedure for evaluating the BER performance under any fading channel where the taps $\{\alpha_l,\tau_{l,0}\}_{l=0}^L$ are treated as random. We recall from (3) that the received signal within each T_s-long interval $t\in[nT_s,(n+1)T_s)$ is given by $r_n(t):=r(t+nT_s)|_{t=0}^{T_s}$, which has the form

$$r_n(t)=\sqrt{\mathcal{E}_s}\left[s(n)h_s(t-\tau)+s(n-1)h_s(t+T_s-\tau)\right]+v_n(t)\qquad t\in[0,T_s).\tag{7}$$

Here, $v_n(t):=v(t+nT_s)|_{t=0}^{T_s}$, and $h_s(t)=\sum_{j=0}^{N_f-1}h(t-jT_f-c_jT_c)$ has been defined to be the T_s-long received symbol template that consists of N_f shifted copies of the composite channel $h(t)=\sum_{l=0}^L\alpha_l p(t-\tau_{l,0})$. The energy of $h_s(t)$ is given by $N_f\mathcal{E}_h$, where $\mathcal{E}_h:=\int_0^{T_f}h^2(t)dt$ contains the channel energy in each frame. The optimal unit-energy correlation template under mistiming is then given by

$$p_r^{(rc)}(t)=\frac{1}{\sqrt{N_f\mathcal{E}_h}}\left[h_s(t-\tau)+h_s(t+T_s-\tau)\right].\quad t\in[0,T_s)\tag{8}$$

which is nothing but a circularly shifted (by τ) version of $h_s(t)$ to confine it within $t\in[0,T_s)$. The decision statistic for $s(n)$ becomes $y(n):=\int_0^{T_s}r_n(t)p_r^{(rc)}(t)dt$, whose signal component is given by $y_s(n)=\sqrt{(\mathcal{E}_s/N_f\mathcal{E}_h)}\left[s(n)\int_\tau^{T_s}h_s^2(t-\tau)dt+s(n-1)\int_0^\tau h_s^2(t-\tau+T_s)dt\right]$. Let us define $\lambda_{h_s}(\tau):=\int_0^\tau h_s^2(t-\tau+T_s)dt=\int_0^\tau dt=int_{T_s-\tau}^{T_s}h_s^2(t)dt\in[0,N_f\mathcal{E}_h]\in[0,N_f\mathcal{E}_h]$, which roughly has N_ϵ times the channel energy $\mathcal{E}_h$. It is difficult to express it in terms of $\mathcal{E}_h$ in an exact form when TH is present. The output $y_s(n)$ can then be simplified as

$$y_s(n)=\sqrt{\mathcal{E}_sN_f\mathcal{E}_h}\left[s(n)\left(1-\frac{\lambda_{h_s}(\tau)}{N_f\mathcal{E}_h}\right)+s(n-1)\frac{\lambda_{h_s}(\tau)}{N_f\mathcal{E}_h}\right].\tag{9}$$

Depending on whether $(s(n),\ s(n-1))$ have the same or opposite signs, the effective sample energy conditioned on one channel realization $h(t)|_{\{\alpha_l\}}$ is given by $\mathcal{E}_\alpha(\epsilon|\{\alpha_l\})=((1/\sqrt{\mathcal{E}_s})y_s(n)|(1,1))^2=N_f\mathcal{E}_h$ subject to tracking errors only, and $\mathcal{E}_\alpha(N_\epsilon,\epsilon|\{\alpha_l\})=((1/\sqrt{\mathcal{E}_s})y_s(n)|(1,-1))^2=N_f\mathcal{E}_h(1-2\lambda_{h_s}(\tau)/(N_f\mathcal{E}_h))^2$ under both acquisition and tracking errors. The general BER expression in (6) still applies, which yields the instantaneous BER under any channel realization $h(t)$

$$\begin{aligned}P_e\left(\tau_0|h(t)\right)&=\frac{1}{2}Q\left(\sqrt{\frac{2\mathcal{E}_sN_f\mathcal{E}_h}{\mathcal{N}_o}}\right)\\&\quad+\frac{1}{2}Q\left(\sqrt{\frac{2\mathcal{E}_sN_f\mathcal{E}_h}{\mathcal{N}_o}\left(1-\frac{2\lambda_{h_s}(\tau)}{N_f\mathcal{E}_h}\right)^2}\right).\end{aligned}\tag{10}$$

Equation (10) applies to both direct-path and multipath channels, regardless of TH. In the absence of TH, (10) can be considerably simplified by noting that $\lambda_{h_s}(\tau)=\int_{(N_f-N_\epsilon)T_f}^{N_fT_f}h_s^2(t)dt+\int_{(N_f-N_\epsilon)T_f-\epsilon}^{(N_f-N_\epsilon)T_f}h_s^2(t)dt$. Introducing an ϵ-dependent ratio $\lambda_h(\epsilon):=(1/\mathcal{E}_h)\int_{T_f-\epsilon}^{T_f}h^2(t)dt\in[0,1]$, we have $\lambda_{h_s}(\tau)=\mathcal{E}_h(N_\epsilon+\lambda_h(\epsilon))$. This indicates that [c.f. (9)] among the total channel energy $N_f\mathcal{E}_h$, the portion that is leaked into the ISI term $s(n-1)$ is proportional to the frame-level offset N_ϵ, subject to certain ϵ-induced variations $\lambda_h(\epsilon)\le 1$. Correspondingly, the instantaneous BER in the absence of TH becomes

$$\begin{aligned}P_e\left(\tau=N_\epsilon T_f+\epsilon|h(t)\right)&=\frac{1}{2}Q\left(\sqrt{\frac{2\mathcal{E}_sN_f\mathcal{E}_h}{\mathcal{N}_o}}\right)\\&\quad+\frac{1}{2}Q\left(\sqrt{\frac{2\mathcal{E}_sN_f\mathcal{E}_h}{\mathcal{N}_o}\left(1-\frac{2\left(N_\epsilon+\lambda_h(\epsilon)\right)}{N_f}\right)^2}\right).\end{aligned}\tag{11}$$

Both (10) and (11) are expressed in terms of a given channel realization $h_s(t)$ or $h(t)$, regardless of the channel type. For any random channel (e.g., [6]–[9]), the average BER can be numerically evaluated by first computing $\mathcal{E}_h$ and $\lambda_{h_s}(\tau)$ (or $\lambda_h(\epsilon)$) for each channel realization $h(t)$, followed by averaging (10) [or (11)] over a large number of realizations. Such a procedure yields $P_e(\tau)=E_{h(t)}\{P_e(\tau|h(t))\}$ for optimum detection.

IV. BER Sensitivity Under Gaussian Fading

In addition to optimum reception using the continuous-time correlation-template $p_r^{(rc)}(t)$ in (8), we are also motivated to evaluate a general correlation-based RAKE receiver, whose parameters L', $\{w_{l'}\}$, and $\{\tilde{\tau}_{l',0}\}$ can be set to reflect design tradeoffs among detection performance, implementation complexity,

[1]Because mistiming gives rise to ISI, an optimal maximum likelihood (ML) detector requires sequence detection. On the other hand, when the receiver is unaware of the existence of mistiming, symbol-by-symbol detection is typically used. The receiver we discuss here is an optimum symbol-by-symbol ML detector under mistiming and a broad-sense optimal ML detector under perfect timing.

and robustness to mistiming. We seek the BER expressions for any RAKE receivers, with respect to the statistics of the random channel parameters $\{\alpha_l\}_{l=0}^{L}$.

Characterizing a fading channel requires knowledge of the joint pdf of the tap fading gains. In a dense multipath environment, paths that are sufficiently far apart can be considered (at least approximately) uncorrelated, even though neighboring paths in a cluster may be correlated. For simplicity, we will assume that all tap gains are mutually uncorrelated, i.e., $E\{\alpha_l\alpha_{l'}\} = E\{\alpha_l^2\}\delta(l-l')$ but not necessarily identically distributed. We focus on Gaussian fading channels, in which each tap α_l is Gaussian distributed with variance $\Omega_l := E\{\alpha_l^2\}$. This assumption is justified by the well-cited statistical channel model in [7], where a bandpass channel is measured to have Gaussian-distributed gains in both the real and imaginary parts, resulting in Rayleigh distributed path envelopes. Since a baseband (carrier-less) UWB channel only has real-valued components, we discard the imaginary portion of the channel model in [7] to deduce that each α_l is Gaussian distributed with zero mean. Being real-valued, $alpha_i$ may take either a positive or a negative sign.

To facilitate our performance analysis, we revisit the general RAKE structure of Fig. 1 and introduce some definitions that will be instrumental to the design of maximal ratio combining (MRC) in the presence of mistiming. Consider, for example, $y_s(n)$ in (5) without TH, i.e., $\{c_j = 0\}$ [c.f. [5, (28)]]

$$y_s(n) = \sqrt{\mathcal{E}_s}\sum_{l'=0}^{L'} w_{l'}\sum_{l=0}^{L}\alpha_l\sum_{q=0}^{1}R_p\left(\Lambda_p(\epsilon,l,l',q)\right) \cdot\left[s(n)\left(1-\frac{N_\epsilon+q}{N_f}\right)+s(n-1)\frac{N_\epsilon+q}{N_f}\right] \quad (12)$$

where $\Lambda_p(\epsilon,l,l',q) := \epsilon+\tau_l-\tilde{\tau}_{l'}-qT_f$. This output can be rewritten as $y_s(n)=\sum_{l'=0}^{L'} w_{l'}y_{s,l'}(n)$, where $y_{s,l'}(n)$ is the noise-free correlation output at the l'th finger, generated by correlating $r(t)-v(t)$ with the time-shifted finger sliding correlator $p_{s,l'}^{(rc)}(t-\hat{\tau}) := p_s(t-\tilde{\tau}_{l',0}-\hat{\tau})$. We suppose the RAKE fingers are sufficiently separated in time (e.g., $\tilde{\tau}_{l'+1,0}-\tilde{\tau}_{l',0}\geq 2T_p, \forall l'$) so that individual finger outputs $y_{s,l'}(n)$ pick out different delayed path(s) (α_l,τ_l) and, thus, are mutually independent across l'. At the l'th RAKE finger, associated with $y_{s,l'}(n)$ conditioned on $(s(n),\, s(n-1))$, $\forall l'$, we define

$$\begin{aligned}\beta_{l'}(\epsilon) &:= \frac{1}{\sqrt{\mathcal{E}_s}}y_{s,l'}(n)\big|(1,1)\\ &= \sum_{l=0}^{L}\alpha_l\sum_{q=0}^{1}R_p\left(\Lambda_p(\epsilon,l,l',q)\right) \quad (13)\\ \beta_{l'}(N_\epsilon,\epsilon) &:= \frac{1}{\sqrt{\mathcal{E}_s}}y_{s,l'}(n)\big|(1,-1)\\ &= \sum_{l=0}^{L}\alpha_l\sum_{q=0}^{1}R_p\left(\Lambda_p(\epsilon,l,l',q)\right)\left(1-\frac{2(N_\epsilon+q)}{N_f}\right). \quad (14)\end{aligned}$$

With (13) and (14), $y(n)$ conditioned on $(s(n),\, s(n-1))$ becomes

$$y(n)\big|(1,1) = \sqrt{\mathcal{E}_s}\sum_{l'=0}^{L'} w_{l'}\beta_{l'}(\epsilon)+v(n) \quad (15)$$

$$y(n)\big|(1,-1) = \sqrt{\mathcal{E}_s}\sum_{l'=0}^{L'} w_{l'}\beta_{l'}(N_\epsilon,\epsilon)+v(n). \quad (16)$$

Observe that $s(n)\neq s(n-1)$ gives rise to effective channel-reception gains $\{\beta_{l'}(N_\epsilon,\epsilon)\}_{l'=0}^{L'}$, which describe the energy capture capability of coherent detectors in the corresponding fingers, characterized by $\mathcal{E}_{\alpha,l'}(N_\epsilon,\epsilon|\{\alpha_l\}_{l=0}^{L}\}) = \beta_{l'}^2(N_\epsilon,\epsilon)$, $l'=0,\ldots,L'$, which are subject to both acquisition and tracking errors. On the other hand, the impact of the acquisition error is alleviated by transmission of identical consecutive symbol pairs $s(n)=s(n-1)$, which leads to different effective channel gains $\{\beta_{l'}(\epsilon)\}_{l'=0}^{L'}$. The energy capture index of the given finger subject to the tracking error only is $\mathcal{E}_{\alpha,l'}(\epsilon|\{\alpha_l\}_{l=0}^{L}\}) = \beta_{l'}^2(\epsilon)$. Note that when the RAKE fingers are matched to the channel path delays, i.e., $\tau_{l,0}=\tilde{\tau}_{l,0}, \forall l$, it follows from (13) and (14) that $\beta_{l'}(0)=\beta_{l'}(0,0)=\alpha_{l'}$ when there is no mistiming. The equivalence of $\beta_{l'}(0)$ and $\beta_{l'}(0,0)$ holds true under perfect timing in any RAKE setup. A critical distinction between perfect timing and mistiming emerges: With perfect timing, there is no ISI when T_f is chosen to be larger than the delay spread with a guard time of T_p, i.e., $T_f\geq\tau_{L,0}+2T_p$, and there is only one set of effective channel gains $\{\beta_{l'}(0)\}_{l'=0}^{L'}$ that connects $y_s(n)$ with $s(n)$. In contrast, mistiming induces ISI, resulting in two sets of effective channel gains $\{\beta_{l'}(N_\epsilon,\epsilon)\}_{l'=0}^{L'}$ and $\{\beta_{l'}(\epsilon)\}_{l'=0}^{L'}$. In practice, channel gain estimation follows the synchronization task. We thus assume that the receiver has perfect knowledge of the channel subject to mistiming (i.e.,$\{\beta_{l'}(N_\epsilon,\epsilon)\}_{l'=0}^{L'}$ and $\{\beta_{l'}(\epsilon)\}_{l'=0}^{L'}$ are available) in order to isolate the impact of mistiming from that of imperfect channel estimation. This assumption is quite different from directly knowing $\{\alpha_l\}_{l=0}^{L}$, which is impossible to obtain without accurate synchronization. Keep in mind that MRC design is based on the available channel estimates.

Deriving the average BER from (15) and (16) relies on the pdfs of the random channel parameters $\{\beta_{l'}(N_\epsilon,\epsilon)\}_{l'=0}^{L'}$ and $\{\beta_{l'}(\epsilon)\}_{l'=0}^{L'}$. Note from (13) and (14) that each of the effective channel gains is a linear combination of Gaussian faded $\{\alpha_l\}_{l=0}^{L}$. Thus, they are also zero-mean Gaussian variables and can be fully characterized by their variances $\bar{\mathcal{E}}_{\alpha,l'}(\epsilon) := E\{\beta_{l'}^2(\epsilon)\} = E\{\mathcal{E}_{\alpha,l'}(\epsilon|\{\alpha_l\})\}$ and $\bar{\mathcal{E}}_{\alpha,l'}(N_\epsilon,\epsilon) := E\{\beta_{l'}^2(N_\epsilon,\epsilon)\} = E\{\mathcal{E}_{\alpha,l'}(\epsilon|\{\alpha_l\})\}$, $\forall l'$, which are given, respectively, by [c.f. (13) and (14)]

$$\bar{\mathcal{E}}_{\alpha,l'}(\epsilon) = \sum_{l=0}^{L}\Omega_l\left(\sum_{q=0}^{1}R_p\left(\Lambda_p(\epsilon,l,l',q)\right)\right)^2 \quad (17)$$

$$\bar{\mathcal{E}}_{\alpha,l'}(N_\epsilon,\epsilon) = \sum_{l=0}^{L}\Omega_l\left(\sum_{q=0}^{1}R_p\left(\Lambda_p(\epsilon,l,l',q)\right) \times\left(1-\frac{2(N_\epsilon+q)}{N_f}\right)\right)^2. \quad (18)$$

TABLE I
AVERAGE ENERGY CAPTURE FOR A SLIDING CORRELATOR

Flat fading	$\bar{\mathcal{E}}_\alpha(\epsilon)=\Omega_0 R_p^2(\epsilon)$
no TH	$\bar{\mathcal{E}}_\alpha(N_\epsilon,\epsilon)=\Omega_0 R_p^2(\epsilon)(1-N_\epsilon/N_f)^2$
Flat fading	$\bar{\mathcal{E}}_\alpha(\epsilon)=\Omega_0 R_p^2(m_oT_c+\epsilon-q_oT_f)\left(\frac{1}{N_f}\sum_{j=0}^{N_f-1}I_{j,q_o}(m_o)\right)^2$
with TH	$\bar{\mathcal{E}}_\alpha(N_\epsilon,\epsilon)=\Omega_0 R_p^2(m_oT_c+\epsilon-q_oT_f)\left(\frac{1}{N_f}\left[\sum_{j=N_\epsilon+q_o}^{N_f-1}I_{j,q_o}(m_o)-\sum_{j=0}^{N_\epsilon+q_o-1}I_{j,q_o}(m_o)\right]\right)^2$
Multipath	$\bar{\mathcal{E}}_\alpha(\epsilon)=\sum_{l=0}^{L}\Omega_l\left(\frac{1}{N_f}\sum_{j=0}^{N_f-1}R_p(\Lambda_p(j,l,q))\right)^2;$
with TH	$\bar{\mathcal{E}}_\alpha(N_\epsilon,\epsilon)=\sum_{l=0}^{L}\Omega_l\left(\sum_{q=0}^{1}\frac{1}{N_f}\left[\sum_{j=N_\epsilon+q}^{N_f-1}R_p(\Lambda_p(j,l,q))-\sum_{j=0}^{N_\epsilon+q-1}R_p(\Lambda_p(j,l,q))\right]\right)^2$ where $\Lambda_p(j,l,q):=(c(j-N_\epsilon-q)-c(j))T_c+\epsilon+\tau_{l,0}-qT_f$

Having obtained the pdfs of the channel taps picked under mistiming, the average BER in fading channels can be obtained by integrating the instantaneous BER expressions in (6) over the joint pdf of these independent random parameters. An equivalent form of the complementary error function $Q(x):=(1/\pi)\int_0^{\pi/2}\exp(-x^2/(2\sin^2\theta))d\theta$, and the results in [10], will be used to facilitate the analysis.

A. Sliding Correlator

We start with a sliding correlator operating in dense multipath. With a single RAKE finger, the normalized correlator weight is always $w_0=\pm 1$, where the sign matches the phase shift of the corresponding channel amplitude α_0. Hence, $\mathcal{E}_\alpha(\epsilon|\{\alpha_l\})=\beta_0^2(\epsilon)$ and $\mathcal{E}_\alpha(N_\epsilon,\epsilon|\{\alpha_l\})=\beta_0^2(N_\epsilon,\epsilon)$, both of which are χ^2-distributed with means $\bar{\mathcal{E}}_\alpha(\epsilon)=\bar{\mathcal{E}}_{\alpha,0}(\epsilon)$ and $\bar{\mathcal{E}}_\alpha(N_\epsilon,\epsilon)=\bar{\mathcal{E}}_{\alpha,0}(N_\epsilon,\epsilon)$. Both quantities can be deduced from (17) and (18) by setting $l'=0$.

Based on the conditional BER in (6), and knowing $\beta_0(\epsilon)$ and $\beta_0(N_\epsilon,\epsilon)$ as Gaussian variables, the average BER can be derived as

$$\begin{aligned}P_e(N_\epsilon,\epsilon)&=\frac{1}{2}\int_0^\infty Q\left(\sqrt{\frac{2\mathcal{E}_s\beta^2}{\mathcal{N}_o}}\right)p_{\beta_0(\epsilon)}(\beta)d\beta\\&\quad+\frac{1}{2}\int_0^\infty Q\left(\sqrt{\frac{2\mathcal{E}_s\tilde{\beta}^2}{\mathcal{N}_o}}\right)p_{\beta_0(N_\epsilon,\epsilon)}(\tilde{\beta})d\tilde{\beta}\\&=\frac{2}{\pi}\int_0^{\frac{\pi}{2}}\frac{1}{4}\left[\sqrt{\left(\frac{2\mathcal{E}_s\bar{\mathcal{E}}_\alpha(\epsilon)}{\mathcal{N}_o\sin^2\theta}+1\right)^{-1}}\right.\\&\qquad\left.+\sqrt{\left(\frac{2\mathcal{E}_s\bar{\mathcal{E}}_\alpha(N_\epsilon,\epsilon)}{\mathcal{N}_o\sin^2\theta}+1\right)^{-1}}\right]d\theta\\&=\frac{1}{2\pi}\left[\arctan\left(\sqrt{\frac{2\mathcal{E}_s\bar{\mathcal{E}}_\alpha(\epsilon)}{\mathcal{N}_o}}^{-1}\right)\right.\\&\qquad\left.+\arctan\left(\sqrt{\frac{2\mathcal{E}_s\bar{\mathcal{E}}_\alpha(\epsilon)}{\mathcal{N}_o}}^{-1}\right)\right].\end{aligned}\tag{19}$$

For sliding-correlator reception, the result in (19) can be applied to other operating scenarios. The key is to identify the corresponding $\bar{\mathcal{E}}_\alpha(\epsilon)$ and $\bar{\mathcal{E}}_\alpha(N_\epsilon,\epsilon)$ from (13) and (14). Such results are summarized in Table I.

B. RAKE Combining

To perform MRC, we select the RAKE multipliers $w_{l'}$ to match the effective channel gains at individual fingers, whereas the channel parameters are estimated symbol by symbol. Under mistiming, when $s(n)=s(n-1)$, the channel gains are affected by the tracking error only, and we set $w_{l'}=c_1^{-1/2}\beta_{l'}(\epsilon)$. On the other hand, when $s(n)\neq s(n-1)$, both acquisition and tracking errors affect symbol detection, and we set $w_{l'}=c_2^{-1/2}\beta_{l'}(N_\epsilon,\epsilon)$. The coefficients $c_1:=\sum_{l'=0}^{L'}\beta_{l'}^2(\epsilon)$ and $c_2:=\sum_{l'=0}^{L'}\beta_{l'}^2(N_\epsilon,\epsilon)$ normalize $w_{l'}$ to ensure $\sum_{l'=0}^{L'}w_{l'}^2=1$. Correspondingly, the overall energy capture indices used in (6) become $\mathcal{E}_\alpha(\epsilon|\{\alpha_l\}_{l=0}^L)=(\sum_{l'=0}^{L'}w_{l'}\beta_{l'}(\epsilon))^2=\sum_{l'=0}^{L'}\beta_{l'}^2(\epsilon)$ and $\mathcal{E}_\alpha(N_\epsilon,\epsilon|\{\alpha_l\}_{l=0}^L)=(\sum_{l'=0}^{L'}w_{l'}\beta_{l'}(N_\epsilon,\epsilon))^2=\sum_{l'=0}^{L'}\beta_{l'}^2(N_\epsilon,\epsilon)$, respectively, both of which are χ^2-distributed. The average BER of MRC reception is thus given by

$$\begin{aligned}&P_e(N_\epsilon,\epsilon)\\&=E_{\{\alpha_l\}}\left\{P_e\left(N_\epsilon,\epsilon|\{\alpha_l\}_{l=0}^L\right)\right\}\\&=\frac{1}{2}E_{\{\beta_{l'}\}}\left\{Q\left(\sqrt{\frac{2\mathcal{E}_s}{\mathcal{N}_o}\sum_{l'=0}^{L'}\beta_{l'}^2(\epsilon)}\right)\right.\\&\qquad\left.+Q\left(\sqrt{\frac{2\mathcal{E}_s}{\mathcal{N}_o}\sum_{l'=0}^{L'}\beta_{l'}^2(N_\epsilon,\epsilon)}\right)\right\}\\&=\frac{1}{2\pi}E_{\{\beta_{l'}\}}\left\{\int_0^{\frac{\pi}{2}}\exp\left(-\frac{\mathcal{E}_s}{\mathcal{N}_o\sin^2\theta}\sum_{l'=0}^{L'}\beta_{l'}^2(\epsilon)\right)d\theta\right\}\\&\quad+\frac{1}{2\pi}E_{\{\beta_{l'}\}}\left\{\int_0^{\frac{\pi}{2}}\exp\left(-\frac{\mathcal{E}_s}{\mathcal{N}_o\sin^2\theta}\sum_{l'=0}^{L'}\beta_{l'}^2(N_\epsilon,\epsilon)\right)d\theta\right\}\\&=\frac{2}{\pi}\int_0^{\frac{\pi}{2}}\frac{1}{4}\left[\prod_{l'=0}^{L'}\sqrt{\left(\frac{2\mathcal{E}_s\bar{\mathcal{E}}_{\alpha,l'}(\epsilon)}{\mathcal{N}_o\sin^2\theta}+1\right)^{-1}}\right.\\&\qquad\left.+\prod_{l'=0}^{L'}\sqrt{\left(\frac{2\mathcal{E}_s\bar{\mathcal{E}}_{\alpha,l'}(N_\epsilon,\epsilon)}{\mathcal{N}_o\sin^2\theta}+1\right)^{-1}}\right]d\theta\end{aligned}\tag{20}$$

which can be computed numerically by treating θ as a random variable uniformly distributed in $[0,\pi/2]$, and evaluating the expectation of the integrand with respect to θ [10].

For MRC-RAKE reception, the result in (20) can be applied to other operating scenarios by identifying the corresponding

TABLE II
AVERAGE ENERGY CAPTURE FOR AN MRC CORRELATOR

Flat fading	$\bar{\mathcal{E}}_{\alpha,l'}(\epsilon) = \Omega_0 R_p^2(\epsilon - \tilde{\tau}_{l',0})$
no TH	$\bar{\mathcal{E}}_{\alpha,l'}(\epsilon) = \Omega_0 R_p^2(\epsilon - \tilde{\tau}_{l',0})(1 - N_\epsilon/N_f)^2$
Flat fading	$\bar{\mathcal{E}}_{\alpha,l'}(\epsilon) = \Omega_0 R_p^2(m_o T_c + \epsilon - \tilde{\tau}_{l',0} - q_o T_f) \left(\frac{1}{N_f}\sum_{j=0}^{N_f-1} I_{j,q_o}(m_o)\right)^2$
with TH	$\bar{\mathcal{E}}_{\alpha,l'}(N_\epsilon,\epsilon) = \Omega_0 R_p^2(m_o T_c + \epsilon - \tilde{\tau}_{l',0} - q_o T_f)\left(\frac{1}{N_f}\left[\sum_{j=N_\epsilon+q_o}^{N_f-1} I_{j,q_o}(m_o) - \sum_{j=0}^{N_\epsilon+q_o-1} I_{j,q_o}(m_o)\right]\right)^2$
Multipath	$\bar{\mathcal{E}}_{\alpha,l'}(\epsilon) = \sum_{l=0}^{L} \Omega_l \left(\sum_{q=-1}^{2} \frac{1}{N_f}\sum_{j=0}^{N_f-1} R_p\left(\Lambda_p(j,l,l',q)\right)\right)^2$
with TH	$\bar{\mathcal{E}}_{\alpha,l'}(N_\epsilon,\epsilon) = \sum_{l=0}^{L}\Omega_l\left(\sum_{q=-1}^{2}\frac{1}{N_f}\left[\sum_{j=N_\epsilon+q}^{N_f-1} R_p(\Lambda_p(j,l,l',q)) - \sum_{j=0}^{N_\epsilon+q-1} R_p(\Lambda_p(j,l,l',q))\right]\right)^2$ where $\Lambda_p(j,l,l',q) := (c(j-N_\epsilon-q) - c(j))T_c + \epsilon + \tau_l - \tilde{\tau}_{l'} - qT_f$

$\{\bar{\mathcal{E}}_{\alpha,l'}(\epsilon)\}_{l'=0}^{L'}$ and $\{\bar{\mathcal{E}}_{\alpha,l'}(N_\epsilon,\epsilon)\}_{l'=0}^{L'}$ of all the RAKE fingers l'. Such results are summarized in Table II.

As a performance benchmark, the average BER for Gaussian fading channels under perfect timing is given from (19) and (20) by setting $\epsilon = 0$ and $N_\epsilon = 0$. The average energy capture indices per finger become

$$\bar{\mathcal{E}}_{\alpha,l'}(\epsilon=0) = \bar{\mathcal{E}}_{\alpha,l'}(N_\epsilon=0,\epsilon=0) = \sum_{l=0}^{L}\Omega_l R_p^2(\tau_{l,0} - \tilde{\tau}_{l',0}). \tag{21}$$

When $\tilde{\tau}_{l'} = \tau_{l'}$ and $\tilde{\tau}_{l'+1,0} - \tilde{\tau}_{l',0} \geq T_p$, $\forall l' \in [0,L]$, we have $\bar{\mathcal{E}}_{\alpha,l'}(0) = \bar{\mathcal{E}}_{\alpha,l'}(0,0) = \Omega_{l'}$. The average BER of an MRC combiner in (20) is reduced to

$$P_e(0,0) = \frac{2}{\pi}\int_0^{\frac{\pi}{2}} \frac{1}{2}\left[\prod_{l=0}^{L}\sqrt{\left(\frac{2\mathcal{E}_s\Omega_l}{\mathcal{N}_o\sin^2\theta}+1\right)^{-1}}\right] d\theta. \tag{22}$$

When $L' = 0$, the BER of a sliding correlator is simplified from (19) to $P_e(0,0) = (1/\pi)\arctan(\sqrt{(2\bar{\mathcal{E}}_s/\mathcal{N}_o)^{-1}})$.

We conclude this section with some remarks on the optimal symbol-by-symbol detector in Section III and the MRC RAKE receiver in Section IV. The optimal detector adopts a correlation-template matched to the channel-dependent receive symbol waveform; thus, it attains optimal matched filtering. The MRC RAKE receiver can be viewed as a discrete-time version of optimal matched filtering sampled by a collection of RAKE fingers, where the correlation templates are shifted versions of the channel-independent transmit symbol waveform $p_s(t)$, but the combining weights are matched to the aggregate channel gains on the corresponding RAKE fingers. The energy capture capability of an MRC RAKE receiver approaches that of an optimal detector when fingers are closely spaced in time delays, whereas a RAKE with a small number of fingers trades performance for reduced implementation complexity. Although other combining techniques may be considered in lieu of MRC, they may be costly to implement for UWB impulse radios. Any coherent receiver will have to at least recover the phase shift (0 or π) of the aggregate channel amplitudes $\{\beta_{l'}\}$ in (13) and (14), which in turn determine the signs of $\{w_{l'}\}$. Since the channel information is required, it is justified to choose MRC over other suboptimal combiners for performance considerations, given the same number of RAKE fingers.

In addition to the BER sensitivity results derived, another key result in this paper is the development of optimal receiver design under mistiming, as described in (8) and (13)–(16). A conventional approach is to borrow the optimal matched filter $h_s(t)$ under perfect timing or directly use the channel information $\{\alpha_l\}$ to construct detection statistics via correlation. Such an approach ignores the presence of mistiming and, thus, has little tolerance to acquisition errors, especially in the presence of TH. In contrast, our matched filter $p_r^{(rc)}(t)$ in (8) and channel information $\{\beta_{l'}\}$ in (13) and (14) are all τ-dependent and, thus, are able to match the received waveform even under mistiming.

V. BER SENSITIVITY FOR PPM

In PPM, the information-bearing symbols $s(k) \in \{0,1\}$ time shift the UWB transmit filter by multiples of the modulation index Δ (on the order of T_p or T_c) to yield the transmitted waveform $u(t)$ as follows:

$$u(t) = \sqrt{\mathcal{E}_s}\sum_{k=0}^{\infty} p_s\left(t - kN_fT_f - s(k)\Delta\right). \tag{23}$$

Reception of PPM signals follows the same correlation principle as in (4), except that the receive template now becomes $\bar{p}_s(t) := p_s(t) - p_s(t-\Delta)$ for a sliding correlator, and $\bar{p}_s^{(rc)}(t) := \sum_{l'=0}^{L'} w_{l'}\bar{p}_s(t - \tilde{\tau}_{l',0})$ for a generic RAKE receiver. For binary PPM, a decision $\hat{s}(n) = 0$ is made when the correlation output $y(n)$ is positive, and $\hat{s}(n) = 1$ when $y(n)$ is negative. We analyze the BER sensitivity to UWB PPM reception based on generalizations from PAM transmissions.

Extending (5) to the PPM signal in (23), a unifying expression for the detection statistic of PPM UWB is given by

$$y(n) = \sqrt{\mathcal{E}_s}\sum_{k=0}^{\infty}\sum_{l=0}^{L}\sum_{l'=0}^{L'}\sum_{i=0}^{N_f-1}\sum_{j=0}^{N_f-1} \times w_{l'}\alpha_l\frac{R_p(\Lambda_p) - R_p(\Lambda_p - \Delta)}{N_f} + \tilde{v}(n) \tag{24}$$

where $\Lambda_p := (k-n)N_fT_f + (i-j)T_f + (c(i)-c(j))T_c + N_\epsilon T_f + \epsilon + \tau_{l,0} - \tilde{\tau}_{l',0} + s(k)\Delta$. The noise variance of $\tilde{v}(n)$ is $\mathcal{N}_o$, which is twice that of the PAM case, due to the use of a differential receiver template.

Consider the no-TH case for clarity. Similar to (12) (c.f. [5, Sec. III.C]), the signal component of (24) can be simplified to

$$y_s(n) = \sqrt{\mathcal{E}_s}\sum_{l'=0}^{L'} w_{l'}\sum_{l=0}^{L}\alpha_l\sum_{q=0}^{1}\left(1 - \frac{N_\epsilon + q}{N_f}\right) \times \bar{R}_p\left(\Lambda_p(n;l,l',q,\Delta)\right)$$

$$+\sqrt{\mathcal{E}_s}\sum_{l'=0}^{L'} w_{l'}\sum_{l=0}^{L}\alpha_l\sum_{q=0}^{1}\frac{N_\epsilon+q}{N_f} \times \bar{R}_p\left(\Lambda_p(n-1;l,l',q,\Delta)\right) \quad (25)$$

where $\Lambda_p(n;l,l',q,\Delta) := \epsilon+\tau_{l,0}-\tilde{\tau}_{l',0}-qT_f+s(n)\Delta$, and $\bar{R}_p(x) := R_p(x)-R_p(x-\Delta)$.

As evidenced by the analysis for PAM, the energy capture indices of each RAKE finger play an important role in assessing the BER performance in fading channels. In generating the finger outputs $y_{s,l'}(n)$, $l' \in [0,L']$, we replace the finger receive-correlation templates with the PPM format $\bar{p}^{(rc)}_{s,l'}(t) := \bar{p}_s(t-\tilde{\tau}_{l',0})$. Unlike PAM, PPM transmissions entail four possible sets of effective channel-reception gains under mistiming, depending on the different symbol-induced pulse-shifting patterns of every consecutive symbol pair $[s(n),\, s(n-1)]$. Mimicking (13) and (14) and letting $\Lambda_p(\epsilon,l,l',q) := \epsilon+\tau_{l,0}-\tilde{\tau}_{l',0}-qT_f$ and $R_p^{\Delta}(\tau) := R_p(\tau+\Delta)-R_p(\tau-\Delta)$, we deduce from (25) the quantities associated with the l'th RAKE finger $l'=[0,L']$, as

$$\begin{aligned}
&\beta_{l'}(\epsilon;0):\\
&\quad=\frac{1}{\sqrt{\mathcal{E}_s}}y_{s,l'}(n)|(0,0)\\
&\quad=\sum_{l=0}^{L}\alpha_l\sum_{q=0}^{1}\bar{R}_p\left(\Lambda_p(\epsilon,l,l',q)\right) \qquad (26)\\
&\beta_{l'}(N_\epsilon,\epsilon;0):\\
&\quad=\frac{1}{\sqrt{\mathcal{E}_s}}y_{s,l'}(n)|(0,1)\\
&\quad=\sum_{l=0}^{L}\alpha_l\sum_{q=0}^{1}\left[\left(1-\frac{2(N_\epsilon+q)}{N_f}\right)\bar{R}_p\left(\Lambda_p(\epsilon,l,l',q)\right)\right.\\
&\qquad\left.+\frac{N_\epsilon+q}{N_f}R_p^{\Delta}\left(\Lambda_p(\epsilon,l,l',q)\right)\right] \qquad (27)\\
&\beta_{l'}(\epsilon;1):\\
&\quad=-\frac{y_{s,l'}(n)|(1,1)}{\sqrt{\mathcal{E}_s}}\\
&\quad=-\sum_{l=0}^{L}\alpha_l\sum_{q=0}^{1}\bar{R}_p\left(\Lambda_p(\epsilon,l,l',q)+\Delta\right)\\
&\quad=\sum_{l=0}^{L}\alpha_l\sum_{q=0}^{1}\left[\bar{R}_p\left(\Lambda_p(\epsilon,l,l',q)\right)\right.\\
&\qquad\left.-R_p^{\Delta}\left(\Lambda_p(\epsilon,l,l',q)\right)\right] \qquad (28)\\
&\beta_{l'}(N_\epsilon,\epsilon;1):\\
&\quad=-\frac{1}{\sqrt{\mathcal{E}_s}}y_{s,l'}(n)|(1,0)\\
&\quad=\sum_{l=0}^{L}\alpha_l\sum_{q=0}^{1}\left[\left(1-\frac{2(N_\epsilon+q)}{N_f}\right)\bar{R}_p\left(\Lambda_p(\epsilon,l,l',q)\right)\right.\\
&\qquad\left.+\left(\frac{N_\epsilon+q}{N_f}-1\right)R_p^{\Delta}\left(\Lambda_p(\epsilon,l,l',q)\right)\right]. \qquad (29)
\end{aligned}$$

In (28) and (29), negative signs are imposed on the channel-gain definitions because a decision $\hat{s}(n)=1$ is made when the signal component $y_s(n)$ is negative. Comparison of (26) and (27) with (28) and (29) indicates that the effective sampled channel gains of 0 and 1 are asymmetric: There is an offset of $\sum_{l=0}^{L}\alpha_l\sum_{q=0}^{1}R_p^{\Delta}(\Lambda_p(\epsilon,l,l',q))$ between both $R_p^{(L,l')}(N_\epsilon,\epsilon;0)$ and $R_p^{(L,l')}(N_\epsilon,\epsilon;1)$, and $R_p^{(L,l')}(\epsilon;1)$ and $R_p^{(L,l')}(\epsilon;1)$. This difference is determined by the pulse shape $R_p^{\Delta}(\Lambda_p)$, which disappears only when $\Lambda_p=0$.

The BER performance of PPM now hinges on the pdfs of the four sets of aggregate channel taps in (26)–(29). When all the channel taps are Gaussian faded, their variances can be obtained from $\{\Omega_l\}_{l=0}^{L}$ based on their linear relationships with $\{\alpha_l\}_{l=0}^{L}$, as in (17) and (18) for the PAM case. These variances characterize the energy capture capability of the corresponding RAKE fingers under mistiming. Specifically, $\bar{\mathcal{E}}_{\alpha,l'}(\epsilon;0)=E\{\beta_{l'}^2(\epsilon;0)\}$ is the energy capture index of detecting $s(n)=0$ under a tracking error only, whereas $\bar{\mathcal{E}}_{\alpha,l'}(N_\epsilon,\epsilon;0)=E\{\beta_{l'}^2(N_\epsilon,\epsilon;0)\}$ is subject to both acquisition and tracking errors. The energy capture capability of detecting $s(n)=1$ is different, which is characterized by either $\bar{\mathcal{E}}_{\alpha,l'}(\epsilon;1)=E\{\beta_{l'}^2(\epsilon;1)\}$ or $\bar{\mathcal{E}}_{\alpha,l'}(N_\epsilon,\epsilon;1)=E\{\beta_{l'}^2(N_\epsilon,\epsilon;1)\}$, depending on the impact of the acquisition error.

With perfect channel estimation, an MRC receiver selects RAKE weights $\{w_{l'}\}$ to match the effective channel gains at individual fingers, i.e., $\{\beta_{l'}(\epsilon;0)\}$, $\{\beta_{l'}(N_\epsilon,\epsilon;0)\}$, $\{\beta_{l'}(\epsilon;1)\}$, or $\{\beta_{l'}(N_\epsilon,\epsilon;1)\}$. Following (20), the average BER in multipath fading becomes

$$\begin{aligned}
P_e(N_\epsilon,\epsilon)&=\frac{1}{4\pi}\int_0^{\frac{\pi}{2}}\left[\prod_{l'=0}^{L'}\sqrt{\left(\frac{\mathcal{E}_s\bar{\mathcal{E}}_{\alpha,l'}(\epsilon;0)}{\mathcal{N}_o\sin^2\theta}+1\right)^{-1}}\right.\\
&\qquad\left.+\prod_{l'=0}^{L'}\sqrt{\left(\frac{\mathcal{E}_s\bar{\mathcal{E}}_{\alpha,l'}(N_\epsilon,\epsilon;0)}{\mathcal{N}_o\sin^2\theta}+1\right)^{-1}}\right]d\theta\\
&\quad+\frac{1}{4\pi}\int_0^{\frac{\pi}{2}}\left[\prod_{l'=0}^{L'}\sqrt{\left(\frac{\mathcal{E}_s\bar{\mathcal{E}}_{\alpha,l'}(\epsilon;1)}{\mathcal{N}_o\sin^2\theta}+1\right)^{-1}}\right.\\
&\qquad\left.+\prod_{l'=0}^{L'}\sqrt{\left(\frac{\mathcal{E}_s\bar{\mathcal{E}}_{\alpha,l'}(N_\epsilon,\epsilon;1)}{\mathcal{N}_o\sin^2\theta}+1\right)^{-1}}\right]d\theta \qquad (30)
\end{aligned}$$

where $\bar{\mathcal{E}}_{\alpha,l'}(\epsilon;0)$, $\bar{\mathcal{E}}_{\alpha,l'}(N_\epsilon,\epsilon;0)$, $\bar{\mathcal{E}}_{\alpha,l'}(\epsilon;0)$, and $\bar{\mathcal{E}}_{\alpha,l'}(N_\epsilon,\epsilon;0)$ are given by the variances of the Gaussian distributed random variables in (26)–(29) and can be deduced similarly to Table II. By choosing different channel and receiver parameters, this general expression applies to various operating conditions, including all the scenarios listed in Table I.

VI. Simulations

Based on the two general BER expressions (19) and (20) for RAKE-1 and RAKE-MRC receivers, we illustrate the BER sensitivity to timing offset $\tau=\tau_0-\hat{\tau}=N_\epsilon T_f+\epsilon$ in Gaussian fading channels, using the same simulation setup discussed in [5], that is, $\mathcal{E}_s/\mathcal{N}_o=8$ db, $N_f=10$, $T_f=10$ ns, $T_p=1$ ns, $N_c=3$, and $T_c=T_f/N_c$, and for multipath: $L=L'=8$,

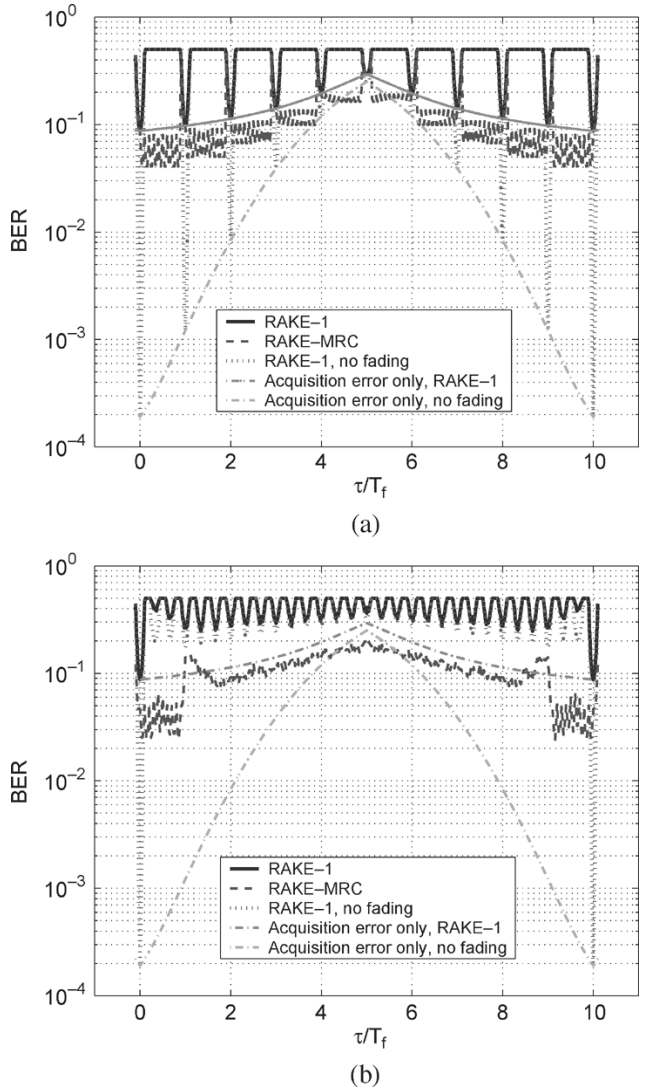

Fig. 2. BER for a direct-path flat fading channel. (a) No TH. (b) With TH.

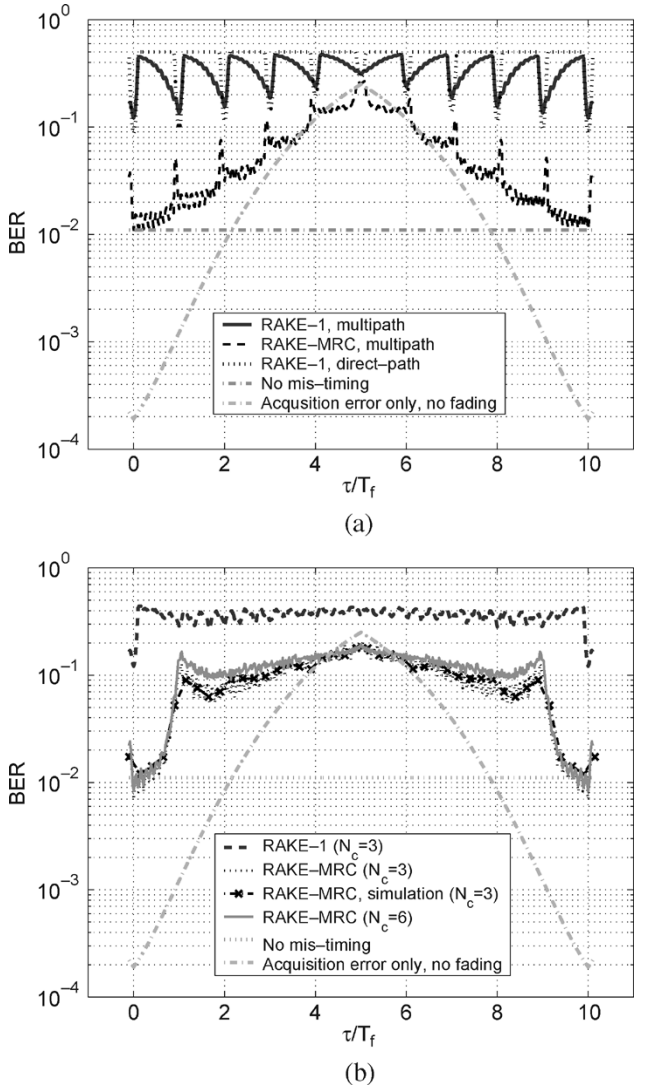

Fig. 3. BER for a multipath fading channel. (a) No TH. (b) With TH.

$\tau_{l,0} = lT_p$, and α_l is Gaussian distributed with variance $\Omega_l = e^{-2l/3}/(\sum_{j=0}^{L} e^{-2j/3})$ for all $l \in [0, L]$ [11]. When an MRC receiver is used, we set $L' = 8$, $\tilde{\tau}_{l'} = l'T_p$, for $l' \in [0, L']$, and the finger weights $\{w_{l'}\}$ are set to be normalized and proportional to the mistimed effective channel gains $\{\beta_{l'}\}$, as explained in Section IV-B. The system parameters are kept reasonably simple to reduce the computational time without losing generality.

BER Sensitivity in Direct-Path Flat-Fading Channels: Without TH, the BER curves for both additive white Gaussian noise (AWGN) and flat-fading channels are plotted in Fig. 2(a) to demonstrate the performance degradation induced by fading. A RAKE-MRC receiver is motivated even for flat-fading channels for the purpose of catching mistimed pulses rather than collecting diversity gain. RAKE-MRC is a discrete-time version of the optimum receiver used in (8), both of which use τ-dependent effective correlation templates to ensure channel matching under mistiming. They are expected to have very close performance in our system setup because RAKE fingers are closely spaced. It is confirmed in Fig. 2 that the use of a RAKE-MRC receiver is able to alleviate the stringent tracking requirements encountered by a RAKE-1 sliding correlator. With TH, the BER comparisons are depicted for RAKE-1 and RAKE-MRC receivers in Fig. 2(b) with reference to RAKE-1 without fading. It is seen that RAKE-MRC is able to collect more effectively the signal energy spread out by TH, thus resulting in better BER. The BER performance gap between AWGN and fading channels could reach levels as high as 20 dB at $\tau = 0$, but the gap is less pronounced as mistiming aggravates, and Gaussian fading appears to be more robust to mistiming when RAKE-MRC is employed.

BER Sensitivity in Dense Multipath Fading Channels: For frequency-selective fading channels with multipath, comparisons are depicted for RAKE-1 and RAKE-MRC in Fig. 3(a), (b). Without TH, the flat-fading case is included as a reference in Fig. 3(a) to demonstrate the multipath spreading effect on symbol detection. The TH effects arise when comparing Fig. 2(b) for a direct-path channel and Fig. 3(b) for a multipath channel. Since TH acts like time shifting similar to multipath spreading, there is no noticeable difference between these two scenarios. On the other hand, when we range the hopping length to be $N_c = 3, 6$, the number of users accommodated increases, but the robustness to mistiming seems to remain stable. For

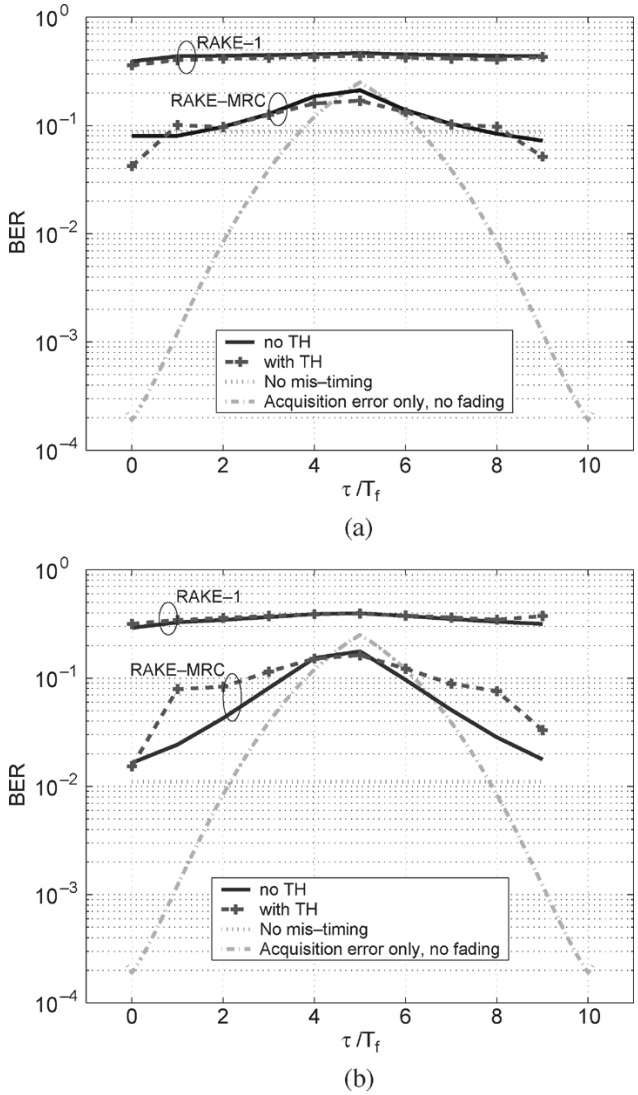

Fig. 4. BER sensitivity to acquisition errors in fading channels. (a) Direct path. (b) Multipath.

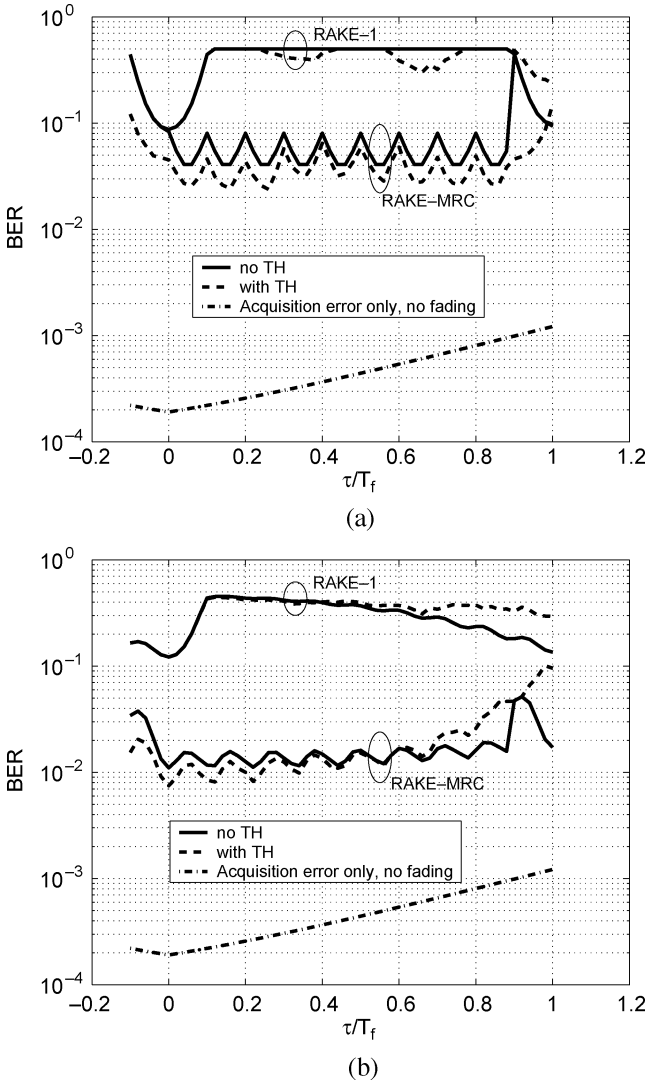

Fig. 5. BER sensitivity to tracking errors in fading channels. (a) Direct path. (b) Multipath.

the most-interesting multipath fading case with TH, we also plotted a BER curve generated by Monte Carlo simulations, which matches well with our analytic curves.

BER Sensitivity to Acquisition: Suppose tracking errors randomly appear over $[-T_p, T_f - T_p]$. The BER sensitivity to acquisition, averaged over a uniformly distributed ϵ, is given by

$$P_e^{acq}(N_\epsilon) := \frac{1}{T_f} \int_{-T_p}^{T_f - T_p} P_e(N_\epsilon, \epsilon) d\epsilon. \tag{31}$$

The acquisition sensitivity for the direct-path and multipath scenarios is illustrated in Fig. 4. It is observed that MRC is needed to sustain acquisition errors, even for flat-fading channels. When TH is present, the BER performance improves over the no-TH case when $N_\epsilon = 0$, due to noise averaging, but appears to be worse when $N_\epsilon \neq 0$, due to the code mismatch. The BER values degrade approximately linearly as the acquisition error increases. Compared with perfect timing, the BER performance in the presence of mistiming is reduced by 2, 4, 7, and 10 dB at $N_\epsilon = 1$, 2, 3, and 4 (with reference to $N_f = 10$), respectively, for PAM transmissions over a 9-tap frequency-selective fading channel. With such a performance degradation, the detection quality quickly becomes unacceptable as N_ϵ increases.

BER Sensitivity to Tracking: If N_ϵ is perfectly acquired, the effect of tracking offset is given by

$$P_e^{trc}(\epsilon) := P_e(N_\epsilon = 0, \epsilon) = \frac{1}{\pi} \int_0^\pi \prod_{l'=0}^{L'} \sqrt{\left(\frac{2\mathcal{E}_s \bar{\mathcal{E}}_{\alpha,l'}(\epsilon)}{\mathcal{N}_o \sin^2\theta} + 1 \right)^{-1}} d\theta. \tag{32}$$

The tracking sensitivity for flat-fading and frequency-selective fading environments is illustrated in Fig. 5. It is obvious that the BER degradation introduced by tracking alone is not drastic in multipath channels, whereas direct-path flat channels have little tolerance to tracking errors when a sliding correlator is employed. These results corroborate also the no-fading case in Part I [5].

BER Sensitivity of PPM versus PAM: To shed light on the comparative behavior between PPM and PAM modulation formats, we plot in Figs. 6(a) and (b) the flat-fading case and the

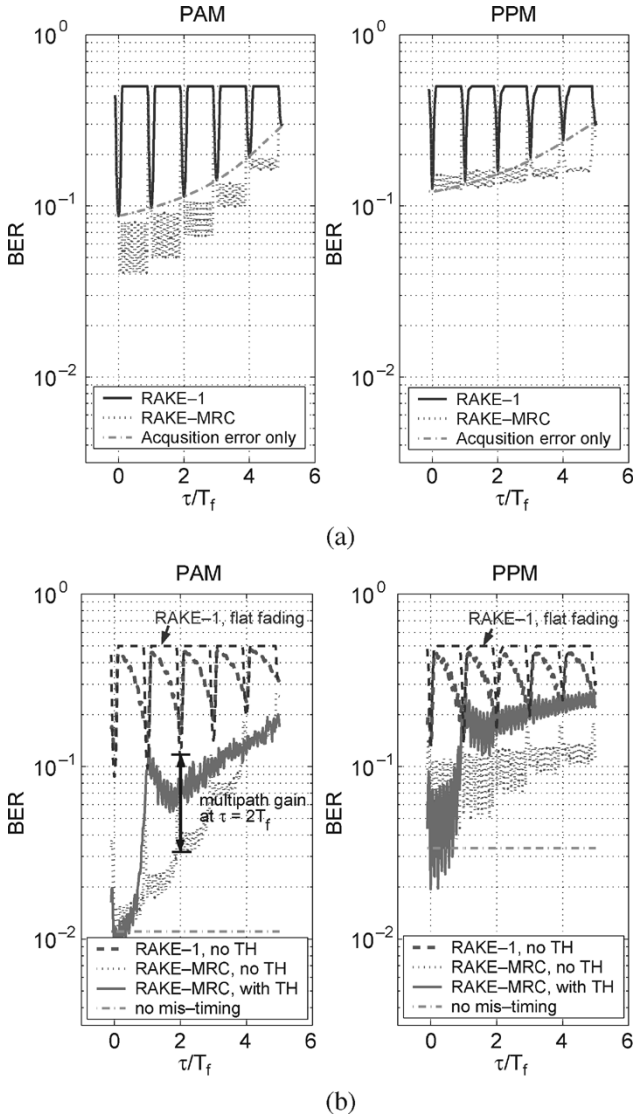

Fig. 6. BER sensitivity to PPM versus PAM in fading channels. (a) Flat fading (no TH). (b) Multipath.

frequency-selective fading case, respectively, all using a PPM modulation index of $\Delta = T_p$. Both figures confirm that PPM is less power efficient than PAM, due to the doubling of sample noise variance when using a differential correlation-template $\bar{p}_s(t)$. For PPM, the general trends of BER sensitivity to mistiming are reminiscent of those of PAM. In the direct-path case, PPM with RAKE-1 reception is very sensitive to tracking errors, exhibiting sharp edges that confine the tracking errors to be $\epsilon \in (-T_p, T_p)$. Under mistiming, RAKE-MRC is suggested for both flat-fading channels and frequency-selective fading channels, in order to improve robustness to mistiming in the former case and to effectively collect diversity gain under mistiming in the latter case. On the other hand, PPM seems to exhibit better robustness to acqsuitision errors. It can be observed that the BER values of PPM degrade more slowly as N_s increases, compared with PAM.

In Table III, we list the BER gains induced by multipath diversity for both PAM and PPM. Compared with transmission over a flat-fading channel, diversity gain is induced when the same transmit energy is spread over multiple propagating paths

TABLE III
BER GAIN INDUCED BY MULTIPATH DIVERSITY

Acquisition error N_ϵ	0	1	2	3	4
PAM: multipath gain (dB)	10	8.4	6.9	4.5	2.3
PPM: multipath gain (dB)	5.4	4.3	3.4	2.9	2.5

and coherently combined at the receiver end; see the contrast between the BER curves of a RAKE-1 receiver in flat fading and that of a RAKE-MRC receiver in frequency-selective fading. Without mistiming, the multipath diversity provided by as many as nine taps in our multipath channel leads to considerable BER improvement of roughly 10 dB for PAM and 5.4 dB for PPM. Unfortunately, the performance advantage is reduced quickly as N_ϵ increases, until reaching a mere gain of 2.3 dB for PAM and 2.5 dB for PPM, at $N_\epsilon = 4$ and 5. The BER diversity gain drops slower for PPM than for PAM.

VII. CONCLUDING SUMMARY

We have demonstrated that UWB transmissions exhibit pronounced sensitivity to mistiming, relative to narrowband single-carrier transmissions. This is attributed in part to the low-duty-cycle nature of UWB signaling, which hinders effective energy capture in the presence of mistiming. The BER performance is dependent on the richness of multipath, the multipath correlation and delay profile, the probabilistic characteristics of the random TH codes employed, as well as the transmit filter parameters T_f, T_p, N_f, N_c, and the receive correlation-template parameters L', $\{\tilde{\tau}_{l'}\}$, and $\{w_{l'}\}$. In particular, direct-path channels have little tolerance to tracking errors, while signal spreading incurred by TH and/or multipath propagation hinders the energy capture capability of optimum RAKE receivers when acquisition offset is present. As shown in Table III, mistiming quickly offsets the diversity gain of UWB as the acquisition error increases for both PAM and PPM. Future investigation could quantify the impact of imperfect channel estimation and multiple-access interference on the performance sensitivity to mistiming. Moreover, TH-UWB has been positioned very early as a possible multiple access technology for UWB. Future trends in the industry may go in different directions [12], which will call for future elaboration on their implications on timing tolerances. It is worth stressing that collection of the diversity gain of UWB in the presence of mistiming requires judicious receiver design. The optimal receivers developed in this paper select the matched filters, or, equivalently, the weighting coefficients of the RAKE, to be dependent on the timing offset. As a result, our RAKE-MRC is relatively robust to mistiming. In contrast, a conventional RAKE-MRC cannot tolerate any timing offset that is more than one pulse width.

ACKNOWLEDGMENT

The authors would like to thank the anonymous reviewers for their constructive comments and suggestions.

REFERENCES

[1] F. Ramirez-Mireles, "On the performance of ultra-wide-band signals in Gaussian noise and dense multipath," *IEEE Trans. Veh. Technol.*, vol. 50, no. 1, pp. 244–249, Jan. 2001.

[2] M. Z. Win and R. A. Scholtz, "Ultra wide bandwidth time-hopping spread-spectrum impulse radio for wireless multiple access communications," *IEEE Trans. Commun.*, vol. 48, no. 4, pp. 679–691, Apr. 2000.
[3] J. Foerster, E. Green, S. Somayazulu, and J. Leeper, "Ultra-wideband technology for short or medium range wireless communications," *Intel Corp. Tech. J.*, 2001. [Online] http://developer.intel.com/technology/itj.
[4] W. M. Lovelace and J. K. Townsend, "The effects of timing jitter and tracking on the performance of impulse radio," *IEEE J. Sel. Areas Commun.*, vol. 20, no. 12, pp. 1646–1651, Dec. 2002.
[5] Z. Tian and G. B. Giannakis, "BER sensitivity to mistiming in ultra-wideband impulse radios—Part I: Modeling," *IEEE Trans. Signal Process.*, vol. 53, no. 4, pp. 1550–1560, Apr. 2005.
[6] H. Lee, B. Han, Y. Shin, and S. Im, "Multipath characteristics of impulse radio channels," in *Proc. IEEE Veh. Technol. Conf.*, Tokyo, Japan, Spring 2000, pp. 2487–2491.
[7] A. A. M. Saleh and R. A. Valenzuela, "A statistical model for indoor multipath propagation," *IEEE J. Sel. Areas Commun.*, vol. JSAC-5, no. 2, pp. 128–137, Feb. 1987.
[8] D. Cassioli, M. Z. Win, and A. F. Molisch, "The ultra-wide bandwidth indoor channel: from statistical model to simulations," *IEEE J. Sel. Areas Commun.*, vol. 20, no. 6, pp. 1247–1257, Aug. 2002.
[9] M. Z. Win and R. A. Scholtz, "Characterization of ultra-wide bandwidth wireless indoor channels: a communication-theoretic view," *IEEE J. Sel. Areas Commun.*, vol. 20, no. 9, pp. 1613–1627, Dec. 2002.
[10] M. K. Simon and M. S. Alouini, *Digital Communications Over Generalized Fading Channels: A Unified Approach to Performance Analysis*. New York: Wiley, 2000.
[11] J. Foerster, "The effects of multipath interference on the performance of UWB systems in an indoor wireless channel," in *Proc. Veh. Tech. Conf.*, 2001, pp. 1176–1180.
[12] IEEE 802.15 WPAN High Rate Alternative PHY Task Group 3a (TG3a). [Online]http://www.ieee802.org/15/pub/TG3a.html

Zhi Tian (M'98) received the B.E. degree in electrical engineering (automation) from the University of Science and Technology of China, Hefei, China, in 1994 and the M. S. and Ph.D. degrees from George Mason University, Fairfax, VA, in 1998 and 2000.

From 1995 to 2000, she was a graduate research assistant with the Center of Excellence in Command, Control, Communications, and Intelligence (C^3I) of George Mason University. Since August 2000, she has been an Assistant Professor with the Department of Electrical and Computer Engineering, Michigan Technological University, Houghton. Her current research focuses on signal processing for wireless communications, particularly on ultrawideband systems.

Dr. Tian serves as an Associate Editor for IEEE TRANSACTIONS ON WIRELESS COMMUNICATIONS. She received a 2003 NSF CAREER award.

Georgios B. Giannakis (F'97) received the Diploma in electrical engineering from the National Technical University of Athens, Athens, Greece, in 1981 and the M.Sc. degree in electrical engineering in 1983, the MSc. degree in mathematics in 1986, and the Ph.D. degree in electrical engineering in 1986, all from the University of Southern California (USC), Los Angeles.

After lecturing for one year at USC, he joined the University of Virginia, Charlottesville, in 1987, where he became a Professor of electrical engineering in 1997. Since 1999, he has been a professor with the Department of Electrical and Computer Engineering, University of Minnesota, Minneapolis, where he now holds an ADC Chair in Wireless Telecommunications. His general interests span the areas of communications and signal processing, estimation and detection theory, time-series analysis, and system identification—subjects on which he has published more than 160 journal papers, 300 conference papers, and two edited books. Current research focuses on transmitter and receiver diversity techniques for single- and multiuser fading communication channels, complex-field and space-time coding, multicarrier, ultrawide band wireless communication systems, cross-layer designs, and distributed sensor networks.

Dr. Giannakis is the (co-) recipient of four best paper awards from the IEEE Signal Processing (SP) Society in 1992, 1998, 2000, and 2001. He also received the Society's Technical Achievement Award in 2000. He served as Editor in Chief for the IEEE SIGNAL PROCESSING LETTERS, as Associate Editor for the IEEE TRANSACTIONS ON SIGNAL PROCESSING and the IEEE SIGNAL PROCESSING LETTERS, as secretary of the SP Conference Board, as member of the SP Publications Board, as member and vice-chair of the Statistical Signal and Array Processing Technical Committee, as chair of the SP for Communications Technical Committee, and as a member of the IEEE Fellows Election Committee. He is currently a member of the the IEEE-SP Society's Board of Governors, the Editorial Board for the PROCEEDINGS OF THE IEEE, and chairs the steering committee of the IEEE TRANSACTIONS ON WIRELESS COMMUNICATIONS.